REPORT DOCUMENTATION PAGE

Form Approved
OMB No. 0704-0188

PLEASE DO NOT RETURN YOUR FORM TO THE ABOVE ADDRESS.

1. REPORT DATE *(DD-MM-YYYY)*	2. REPORT TYPE	3. DATES COVERED *(From - To)*
11/28/2007	Progress Report	June 30, 2007 - November 28, 2007

4. TITLE AND SUBTITLE

Progress Report on the Use of SIG Algorithms in Sea Tests

5a. CONTRACT NUMBER

N00014-06-C-0026

5b. GRANT NUMBER

5c. PROGRAM ELEMENT NUMBER

6. AUTHOR(S)

Lawrence Carin and Patrick Rabenold

5d. PROJECT NUMBER

5e. TASK NUMBER

5f. WORK UNIT NUMBER

7. PERFORMING ORGANIZATION NAME(S) AND ADDRESS(ES)

Signal Innovations Group
1009 Slater Road, Suite 200
Durham, NC 27703

8. PERFORMING ORGANIZATION REPORT NUMBER

CDRL A004

9. SPONSORING/MONITORING AGENCY NAME(S) AND ADDRESS(ES)

Office of Naval Research
875 N. Randolph Street, Suite 1425
Arlington, VA 22203-1995

10. SPONSOR/MONITOR'S ACRONYM(S)

ONR

11. SPONSOR/MONITOR'S REPORT NUMBER(S)

CDRL A004

12. DISTRIBUTION/AVAILABILITY STATEMENT

Statement A

13. SUPPLEMENTARY NOTES

14. ABSTRACT

This report summarizes recent progress by Signal Innovations Group (SIG) in supporting the Naval Research Laboratory (NRL) on the development and application of mine identification algorithms using a Low Frequency Broadband (LFBB) sonar system. SIG has the tasks of developing the algorithms and transitioning them to NRL for use in sea tests. Fully-transitioned algorithms have performed well in sea tests, with additional development increasing the computational efficiency. The discussion below provides a summary of the following items: the Kernel Matching Pursuits (KMP) classification algorithm, the correlation kernel method, and sample results from an NRL sea test.

15. SUBJECT TERMS

16. SECURITY CLASSIFICATION OF:			17. LIMITATION OF ABSTRACT	18. NUMBER OF PAGES	19a. NAME OF RESPONSIBLE PERSON
a. REPORT	b. ABSTRACT	c. THIS PAGE			Larry Carin
U	U	U	UU	11	19b. TELEPHONE NUMBER *(Include area code)* (919) 323-3453

Progress Report on the Use of SIG Algorithms in Sea Tests

Lawrence Carin and Patrick Rabenold
Signal Innovations Group, Inc.
Durham, NC

28 November 2007

This report summarizes recent progress by Signal Innovations Group (SIG) in supporting the Naval Research Laboratory (NRL) on the development and application of mine identification algorithms using a Low Frequency Broadband (LFBB) sonar system. SIG has the tasks of developing the algorithms and transitioning them to NRL for use in sea tests. Fully-transitioned algorithms have performed well in sea tests, with additional development increasing the computational efficiency. The discussion below provides a summary of the following items: the Kernel Matching Pursuits (KMP) classification algorithm, the correlation kernel method, and sample results from an NRL sea test.

I. Kernel Matching Pursuits

A short historical outline of the identification approaches used by the LFBB program is given to set the stage for the present algorithm descriptions and discussion. The first identification algorithms were based on hidden Markov models (HMM). Markov models are effective tools for representing sequential data and, in our application, predict the probability that sequential target strength data is from a particular object. The sequential target strength data is obtained as the autonomous underwater vehicle (AUV) transits past an unknown object. This approach is *generative*, i.e. the modeling of targets and clutter are done without knowledge of the other and identification is effected by choosing the model that best matches the unknown data. The next set of identification approaches explored was *discriminative*, i.e. the data from targets and clutter are simultaneously considered to determine the best boundary that separates targets from clutter. Here a series of Bayesian identification algorithms known as *kernel* algorithms are considered: the support vector machine (SVM), the relevance vector machine (RVM), and the kernel matching pursuits (KMP). All of these *kernel* identification algorithms have very similar performance when applied to the LFBB data. The transition from the SVM to the RVM/KMP was primarily motivated by compactness of the RVM/KMP solutions, which are better suited for implementation on an AUV. The RVM arrives at a compact solution by starting with all of the training data and then pruning data to form a compact solution. The KMP starts with none of the training data and builds up to a compact solution. The KMP was chosen over the RVM because building up a compact solution is more computationally efficient. The KMP algorithm was initially implemented in a way that treats each target aspect as being independently drawn from an identical underlying distribution. Unlike the HMM, this approach results in a trained classifier that ignores any correlation between sequential target responses. This motivated the design of a correlation-based KMP kernel that combines the advantages of a *discriminative* approach and the sequential nature of the data. The structure of the KMP algorithm used in the sea tests is discussed below for a generalized kernel function.

The basic kernel matching pursuits (KMP) algorithm implements a set of functions of the form

$$f_n(\mathbf{x}) = \sum_{i=1}^{n} w_{n,i} K(\mathbf{c}_i, \mathbf{x}) + w_{n,0} = \mathbf{w}_n^T \boldsymbol{\phi}_n(\mathbf{x}) \tag{1}$$

where $w_{n,0}$ is the bias term, $K(\cdot,\cdot)$ is the kernel

$$\boldsymbol{\phi}_n(\cdot) = [1, K(\mathbf{c}_1, \cdot), K(\mathbf{c}_2, \cdot), ..., K(\mathbf{c}_n, \cdot)]^T \tag{2}$$

with $K(\mathbf{c}_i, \cdot)$ the kernel-induced basis function centered at $\mathbf{c}_i$,

$$\mathbf{w}_n = [w_{n,0}, w_{n,1}, w_{n,2}, \cdots, w_{n,n}]^T \tag{3}$$

are the weights that combine the basis functions in the summation, and the subscript *n* is used to denote the number of basis functions being used. This is the same form as found for the support vector machine (SVM) and relevance vector machine (RVM), although for the SVM $K(\mathbf{c}_i, \mathbf{x})$ must be a Mercer kernel, while for the RVM and KMP this is not necessary. We use the KMP instead of the RVM or SVM because of the fact that the KMP has complexity that is linear in the number of training samples. The linear relationship between the amount of training data and the computational effort is key in allowing the LFBB program to process the large amount of training data needed for a blind test or real world operations. A detailed outline of the KMP algorithm is given below.

Assume we are given a training set $\{\mathbf{x}_i, y_i\}_{i=1}^N$ of size *N*, where $\mathbf{x}_i$ is the *i*-th input and y_i its expected output, the weighted sum of squared errors between the expected output and the KMP output is

$$\begin{aligned} e_n &= (1/\textstyle\sum_{i=1}^N \beta_i) \sum_{i=1}^N \beta_i [y_i - f_n(\mathbf{x}_i)]^2 \\ &= (1/\textstyle\sum_{i=1}^N \beta_i) \sum_{i=1}^N \beta_i [y_i - \mathbf{w}_n^T \boldsymbol{\phi}_n(\mathbf{x}_i)]^2 \end{aligned} \tag{4}$$

where β_i is a constant responsible for the importance of the *i*-th training sample ($\mathbf{x}_i$, y_i). For example, $1/\beta_i$ may represent the variance of the *i*th measurement. In addition, if one has *a priori* knowledge that some data $\mathbf{x}_i$ are "better" representative of the system being modeled, this can be accounted for in the parameter β_i. The unknowns in equation (4) are the centers $\mathbf{c}_i$ of the basis functions in $\boldsymbol{\phi}_n$, and the weights are represented by $\mathbf{w}_n$. The determination of $\mathbf{c}_i$ is addressed separately below. At the moment we

suppose $\mathbf{c}_i$ and consequently $\boldsymbol{\phi}_n$ are known and aim at solving for $\mathbf{w}_n$. Then the value of $\mathbf{w}_n$ that minimizes equation (4) is easily found to be

$$\mathbf{w}_n = \mathbf{M}_n^{-1}\{\beta_i \boldsymbol{\phi}_{n,i} y_i\}_i \tag{5}$$

where $\boldsymbol{\phi}_{n,i}$ is an abbreviation of $\boldsymbol{\phi}_n(\mathbf{x}_i)$, $\{\cdot\}_i \overset{Def}{=} \sum_{i=1}^{N}(\cdot)$, and

$$\mathbf{M}_n = \sum_{i=1}^{N} \beta_i \boldsymbol{\phi}_n(\mathbf{x}_i)\boldsymbol{\phi}_n^T(\mathbf{x}_i) = \{\beta_i \boldsymbol{\phi}_{n,i}\boldsymbol{\phi}_{n,i}^T\}_i \tag{6}$$

is the Fisher information matrix.

According to the definition in equation (1), the (n+1)-th order KMP is inductively written as

$$f_{n+1}(\mathbf{x}) = \mathbf{w}_{n+1}^T \boldsymbol{\phi}_{n+1}(\mathbf{x}) \tag{7}$$

where

$$\begin{aligned}\boldsymbol{\phi}_{n+1}(\cdot) &= [1, K(\mathbf{c}_1,\cdot), K(\mathbf{c}_2,\cdot),..., K(\mathbf{c}_n,\cdot), K(\mathbf{c}_{n+1},\cdot)]^T \\ &= \begin{bmatrix} \boldsymbol{\phi}_n(\cdot) \\ \phi_{n+1}(\cdot) \end{bmatrix}\end{aligned} \tag{8}$$

with $\phi_{n+1}(.) = K(\mathbf{c}_{n+1},.)$ a new basis function centered at $\mathbf{c}_{n+1}$. The weighted sum of squared errors of the (n+1)-th order KMP is

$$e_{n+1} = (1/\sum_{i=1}^{N}\beta_i)\sum_{i=1}^{N}\beta_i[y_i - f_{n+1}(\mathbf{x}_i)]^2 \tag{9}$$

Assuming the basis functions in ϕ_{n+1} are all known, then from equation (5)

$$\mathbf{w}_{n+1} = \mathbf{M}_{n+1}^{-1}\{\beta_i \boldsymbol{\phi}_{n+1,i} y_i\}_i \tag{10}$$

minimizes equation (9), where the Fisher information matrix $\mathbf{M}_{n+1}$ is given as

$$\mathbf{M}_{n+1} = \{\beta_i^2 \boldsymbol{\phi}_{n+1,i}\boldsymbol{\phi}_{n+1,i}^T\}_i \tag{11}$$

One may show that $\mathbf{w}_{n+1}$ and e_{n+1} are respectively related to $\mathbf{w}_n$ and e_n as

$$\begin{aligned}&\mathbf{w}_{n+1} = \\ &\begin{bmatrix} \mathbf{w}_n + \mathbf{M}_n^{-1}\{\beta_i \boldsymbol{\phi}_{n,i}\phi_{n+1,i}\}_i b^{-1}[\{\beta_i \boldsymbol{\phi}_{n,i}^T \phi_{n+1,i}\}_i \mathbf{w}_n - \{\beta_i \phi_{n+1,i} y_i\}_i] \\ -b^{-1}\{\beta_i \boldsymbol{\phi}_{n,i}^T \phi_{n+1,i}\}_i \mathbf{w}_n + b^{-1}\{\beta_i \phi_{n+1,i} y_i\}_i \end{bmatrix}\end{aligned} \tag{12A}$$

$$e_{n+1} = e_n - \delta e(K, \mathbf{c}_{n+1}) \tag{12B}$$

where

$$\delta e(K, \mathbf{c}_{n+1}) = (1/\sum_{i=1}^{N} \beta_i) b^{-1} [\{\beta_i \boldsymbol{\phi}_{n,i}^T \phi_{n+1,i}\}_i \mathbf{w}_n - \{\beta_i \phi_{n+1,i} y_i\}_i]^2 \tag{13}$$

and

$$b = \{\beta_i \phi_{n+1,i}^2\}_i - \{\beta_i \phi_{n+1,i} \boldsymbol{\phi}_{n,i}^T\}_i \mathbf{M}_n^{-1} \{\beta_i \boldsymbol{\phi}_{n,i} \phi_{n+1,i}\}_i \tag{14}$$

with $\phi_{n+1,i} = K(\mathbf{c}_{n+1}, \mathbf{x}_i)$. One may show that b^{-1} is a diagonal element of $\mathbf{M}_{n+1}^{-1}$. With sufficient training data points, we can always make $\mathbf{M}_{n+1}$ positive definite, as can be seen from equation (6). Then $\mathbf{M}_{n+1}^{-1}$ is also positive definite and it holds $b^{-1} > 0$, which guarantees $\delta e(K, \mathbf{c}_{n+1})$ is always greater than zero. Therefore, from equation (12B), $e_{n+1} < e_n$, which means appending a new basis function to the KMP generally leads to decrease of the representation error.

As $\delta e(K, \mathbf{c}_{n+1})$ is dependent on the center $\mathbf{c}_{n+1}$ of the new basis function, we obtain different values of $\delta e(K, \mathbf{c}_{n+1})$ by selecting different $\mathbf{c}_{n+1}$. If we confine $\mathbf{c}_{n+1}$ to be selected from the training data, we then can conduct a "greedy" search in the training set but with the previously selected data excluded to avoid repetition, and select the datum that maximizes equation (13). Formally, we have

$$\mathbf{c}_{n+1} = \mathbf{x}_{i_{n+1}} = \arg\max_{\substack{k \neq i_1, \ldots, i_n \\ 1 \le k \le N}} \delta e(K, \mathbf{x}_k) \tag{15}$$

After $\mathbf{c}_{n+1}$ is determined, we update the weights using equation (12A) and the Fisher information matrix using equations (11) and (8).

From equation (13), $\delta e(K, \mathbf{c}_{n+1})$ depends on the form of the kernel $K(\cdot, \cdot)$ as well as on $\mathbf{c}_{n+1}$. This allows us to optimize the kernel to gain further error reduction. A simple approach to take is to first do a "greedy" search of $\mathbf{c}_{n+1}$ in the training set, for a fixed kernel, and then fix $\mathbf{c}_{n+1}$ and optimize the parameters of the kernel. For radial basis function (RBF) kernels, the only parameter other than $\mathbf{c}_{n+1}$ is the kernel width σ, thus optimization of RBF kernels with $\mathbf{c}_{n+1}$ fixed is a one-dimensional search to optimize σ. It is also possible to optimize $\mathbf{c}_{n+1}$ and the kernel width σ simultaneously, but then $\mathbf{c}_{n+1}$ is treated as a free parameter and no longer confined to the training set. Another possibility is optimization over kernels of different functional forms, which offers greater diversity of the set of functions able to be implemented by the KMP.

For the *M*-class classification problem, one builds *M* models defined in equation (1). Suppose the training samples are $\{\mathbf{x}_i, y_i\}_{i=1}^N$ where $\mathbf{x}_i$ is an observed datum and $y_i \in \{1,2,...,M\}$ is its target label. One re-labels the training data for each of the *M* models in the following way. Let the labels for the *m*-th model be denoted as $y_i^{(m)}$, $i = 1,2,...,N$, then

$$y_i^{(m)} = \begin{cases} 1, & \text{if } y_i = m \\ 0, & \text{otherwise} \end{cases} \tag{16}$$

The learning is based on simultaneous minimization of the empirical risks for the *M* models. Thus the cost function of the KMP in the classification case is

$$e_n = (1/\sum_{i=1}^N \beta_i)\sum_{m=1}^M \sum_{i=1}^N \beta_i [y_i^{(m)} - \boldsymbol{\phi}_n^T(\mathbf{x}_i)\mathbf{w}_n^{(m)}]^2 \tag{17}$$

Note that the *M* models have their own weights but share the same basis functions. As in the case of the basic KMP, we first solve for the weights assuming the basis functions (kernel parameters) are fixed. This is done by taking derivative of equation (17) with respect to $\mathbf{w}_n^{(m)}$, setting the result to zero, and solving for $\mathbf{w}_n^{(m)}$

$$\mathbf{w}_n^{(m)} = \mathbf{M}_n^{-1}\{\boldsymbol{\phi}_{n,i} y_i^{(m)}\}_i \tag{18}$$

where $\mathbf{M}_n$ is the same as in equation (6). Following the same methods that were used to derive equation (12), we obtain

$$\mathbf{w}_{n+1}^{(m)} = \begin{bmatrix} \mathbf{w}_n^{(m)} + \mathbf{M}_n^{-1}\{\beta_i \boldsymbol{\phi}_{n,i}\phi_{n+1,i}\}_i b^{-1}[\{\beta_i \boldsymbol{\phi}_{n,i}^T \phi_{n+1,i}\}_i \mathbf{w}_n^{(m)} - \{\beta_i \phi_{n+1,i} y_i^{(m)}\}_i] \\ -b^{-1}\{\beta_i \boldsymbol{\phi}_{n,i}^T \phi_{n+1,i}\}_i \mathbf{w}_n^{(m)} + b^{-1}\{\beta_i \phi_{n+1,i} y_i^{(m)}\}_i \end{bmatrix} \tag{19A}$$

and

$$e_{n+1} = e_n - \delta e(K, \mathbf{c}_{n+1}) \tag{19B}$$

where

$$\delta e(K, \mathbf{c}_{n+1}) = (1/\sum_{i=1}^N \beta_i) b^{-1} \sum_{m=1}^M [\{\beta_i \boldsymbol{\phi}_{n,i}^T \phi_{n+1,i}\}_i \mathbf{w}_n^{(m)} - \{\beta_i \phi_{n+1,i} y_i^{(m)}\}_i]^2 \tag{20}$$

with *b* the same as in equation (14). The learning of KMP classifiers proceeds in a similar generative way as described above. At the *n*-th iteration, we first select $\mathbf{c}_{n+1}$ from the training data set (with the previously selected data excluded) that maximizes equation (20), to locate the new basis function, and

then use equation (19A) to update the weights. We can similarly optimize the kernels in the KMP *M*-ary classifiers, using equation (20) as the objective function to optimize kernel parameters or select different kernel functional forms.

An important observation from the above procedure is that we have not employed a link function to extend the regression problem to classification. Link functions have been employed in the RVM method. We do not employ a link function here because the simple and importantly iterative form of the solution in equations (19) and (20) is driven by the linear model in equation (1). This linearity is lost by introducing a link function. Note that for the *M*-ary classification problem discussed above we drive the label $y_m(\mathbf{x}_i)$ to unity if the $\mathbf{x}_i$ is associated with class *m*, and it is fit to zero otherwise, with this solved jointly for all *M* classes, yielding the weights in equation (19A). A careful examination of the RVM, for example, yields the recognition that $y_m(\mathbf{x}_i)$ is driven toward a large positive number if $\mathbf{x}_i$ corresponds to class *m*, and it is driven toward a large negative number otherwise. In this sense the approach discussed above is closely related to the RVM, and the choice of numbers other than zero and one in equation (16) simply reflects a scaling of the weights. In this sense the KMP and RVM treatment of the *M*-ary classification problem are closely related. The main distinction is that, by employing a link function, the RVM yields a classification as well as a probabilistic measure of confidence (in terms of a number between zero and one) in that classification.

II. Correlation Kernel

A correlation-based kernel has produced the most successful classification results tested thus far. Therefore, this method was implemented in the sea tests as described below. The correlation kernel is characterized by the direct processing of contiguous sets of angle-dependent frequency-domain signatures, without explicit feature extraction. Figure 1 illustrates the process. Given a set of target complex frequency responses $\{\boldsymbol{r}_m\}_{m=1}^{M}$ obtained at *M* regular aspect intervals around a target, unwanted frequency bands are initially filtered out of the spectrum (see Figure 1(a)). The remaining frequency bands taken over a span of 2θ degrees of adjacent target response angles are now employed directly within the kernel. We define a two-dimensional *spectral sequence* centered at aspect *n*, $\boldsymbol{s}_n = \left[\boldsymbol{r}_{n-\theta} \ldots . \boldsymbol{r}_n \ldots . \boldsymbol{r}_{n+\theta}\right]$, where $\boldsymbol{s}_n$ is a $F \times (2\theta + 1)$ data matrix (see Figures 1(b) and 1(c)). We obtain *N* spectral sequences centered at a uniform increment over the range of *M* regular aspect intervals.

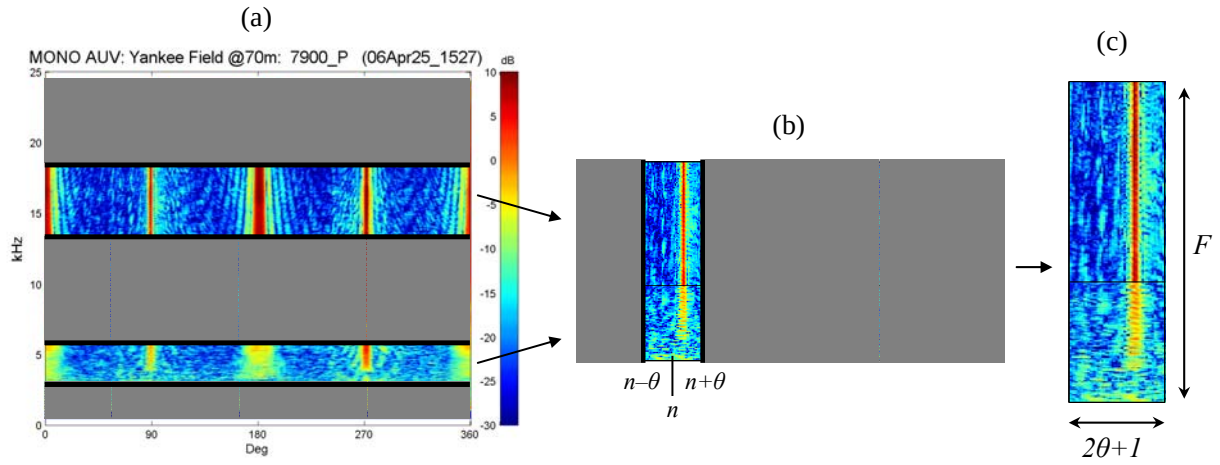

Figure 1 — Data processing for multi-aspect KMP with a correlation kernel. Unwanted frequency bands are filtered out of the sequence of target aspects in (a), the aspects are then divided into spectral sequences (b), in which a single sequence becomes a feature matrix (c).

For a set of spectral sequences, $\{\boldsymbol{s}_n\}_{n=1}^{N}$, the multi-aspect KMP kernel is defined as

$$K(\mathbf{s}_i,\mathbf{s}_j) = e^{-d^2/2\sigma^2}, \tag{21}$$

where $d = \dfrac{1-corr(\mathbf{s}_i,\mathbf{s}_j)}{corr(\mathbf{s}_i,\mathbf{s}_j)}$ is a measure of distance between two spectral sequences based on a correlation coefficient. The correlation is performed only along the aspect dimension (i.e., one strip is slid over the other along the aspect axis and the correlation is calculated at every shift). Efficient numerical computation of the correlation is achieved through the use of fast Fourier transforms. Let $\boldsymbol{S}_i$ and $\boldsymbol{S}_j$ represent two spectral sequences for which one-dimensional FFTs have been computed along the aspect direction for each frequency *f*. Formally, we have $\boldsymbol{S}_i(f,v) = \sum_{\alpha=1}^{2\theta+1} \boldsymbol{s}_i(f,\alpha) e^{-\frac{2\pi v\alpha}{(2\theta+1)}i}$, and the raw correlation, $\gamma(\alpha)$, is computed as

$$\gamma(\alpha) = \sum_{f=1}^{F}\sum_{v=1}^{2\theta+1} \boldsymbol{S}_i(f,v) \times \boldsymbol{S}_j^{*}(f,v) e^{\frac{2\pi v\alpha}{(2\theta+1)}i}, \tag{22}$$

which results in a correlation value at each shift angle α. Taking the maximum shift correlation and normalizing by the energy of the spectral sequences, we have

$$corr(\mathbf{s}_i, \mathbf{s}_j) = \frac{\max_{\alpha} |\gamma(\alpha)|}{\sqrt{\max_{\alpha} \left| \sum_f \mathbf{s}_i^2(f,\alpha) \right|} \sqrt{\max_{\alpha} \left| \sum_{f'} \mathbf{s}_j^2(f,\alpha) \right|}} . \quad (23)$$

The above expression, the absolute correlation coefficient between two signal sequences, lies between 0 and 1 (with 0 being no correlation, and 1 representing perfect correlation between two sequences). Given the kernel defined in equation (21), the KMP algorithm obtains a set of basis functions and the associated weights, where each basis function corresponds to a spectral sequence of contiguous aspects, rather than single-aspect observations in traditional KMP or RVM.

In the testing phase, our objective is to obtain the probability or likelihood of a given unlabeled sequence of target responses belonging to any target or target class. In generative training, each target is associated with a parametric likelihood model, whereas for the discriminative case, we obtain a classifier between two or more targets. Given an unlabeled sequence, we obtain the set of spectral sequences similar to the training phase. The probability of the single sequence belonging to a "trained" target class is given by

$$p(\boldsymbol{s}_{test} \mid \text{target} = j) = w_0^j + \sum_{i=1}^{b_j} w_i^j K(\boldsymbol{s}_{test}, \boldsymbol{s}_i^j), \quad (24)$$

where $\boldsymbol{w}^j = \{w_0^j .... w_{b_j}^j\}$ represents the weight vector corresponding to target j, and $\{\boldsymbol{s}_i^j\}_{i=1}^{b_j}$ represent the corresponding basis functions. Note that $\boldsymbol{s}_{test}$ and $\boldsymbol{s}_i^j$ need to be the same size and the parameter b_j denotes the number of basis functions used for target *j*.

III. Sea Test Results

NRL has performed several sea tests with successful mine identification results. However, the feature extraction and correlation calculations are computationally intensive. The data collected from a sea test generates thousands of test objects, which makes near-real time analysis challenging. Additional development has greatly improved the computational efficiency of the algorithms. Figure 2 illustrates the reduction in discriminative training execution time achieved by optimizing the correlation computations, without altering the computed results. The increase in processing speed is dependent upon several algorithm parameters, such as the size of the frequency bands, *F*, and the number of adjacent angles per spectral sequence, 2θ (see Figure 1(c)). In general, the total execution time for complete training and testing has been reduced by 50-75%.

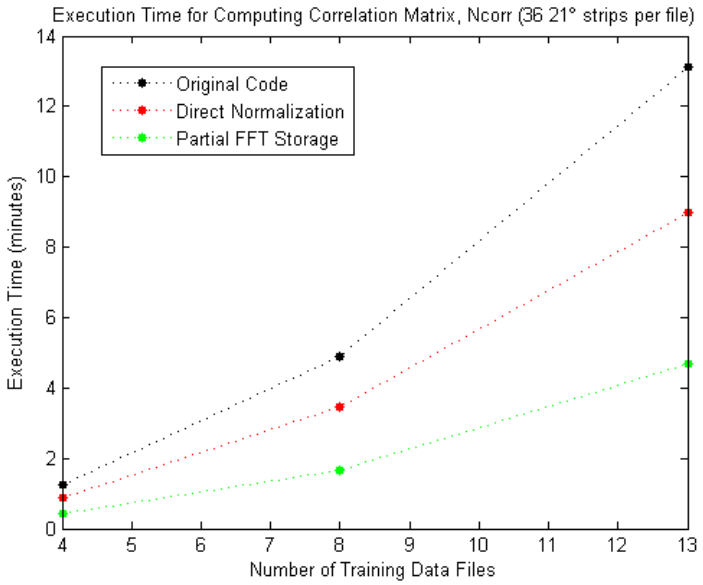

Figure 2 — Execution time as a function of the number of 360º training data files. The black dots represent the original code, while the red and green dots represent added algorithmic optimizations.

In May 2007, NRL performed a sea test off the coast of Corpus Christi, Texas. The following sea test results were produced by using a 4-23kHz frequency band and a $2\theta = 90^{\circ}$ sequence of angles. Figure 3 displays the results of Blind Test 1 with the AUV traversing north and south lines. Approximately 1500 objects (the blue dots) were classified by the algorithm. The classification algorithm perfectly identified the location of every cylindrical mine, while the stealthy targets proved more challenging. Similar results were achieved on additional blind tests.

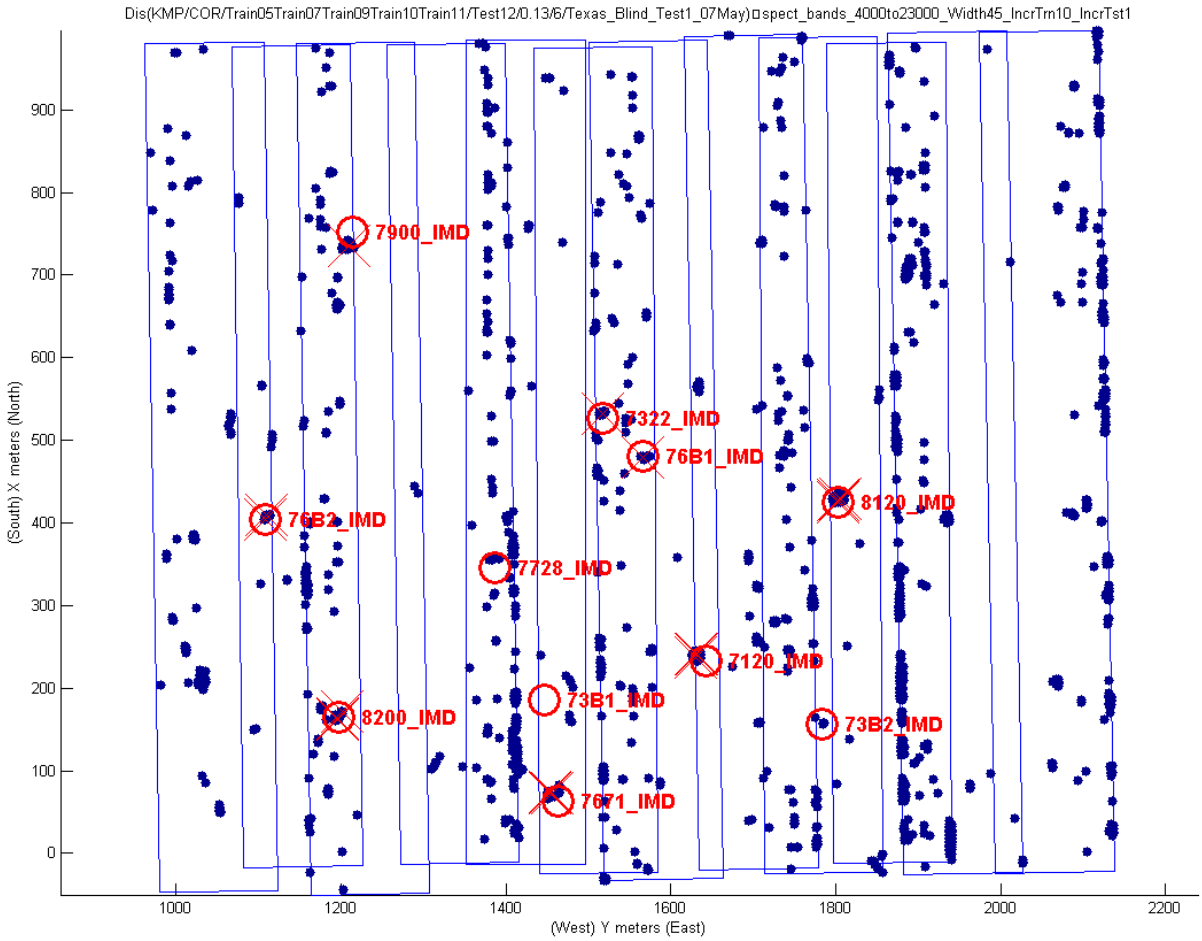

Figure 3 — Mine identification on the Corpus Christi Blind Test 1 north/south lines. The blue dots represent all objects tested. The red circles indicate the known types and locations of mines. A red X marks an object identified as a mine based on the results of the classification algorithm.